Journal of Neuroradiology 000 (2021) 1–8

Available online at ScienceDirect www.sciencedirect.com

Elsevier Masson France EM|consulte www.em-consulte.com

Original Article

The effect of a post-scan processing denoising system on image quality and morphometric analysis

Noriko Kanemaru*, Hidemasa Takao, Shiori Amemiya, Osamu Abe

Department of Radiology, University of Tokyo, Tokyo, Japan

ARTICLE INFO

Article History:
Available online xxx

Keywords:
Cortical thickness
Denoising
FreeSurfer
Magnetic resonance imaging
Morphometry
Surface-based morphometry

ABSTRACT

Purpose: MR image quality and subsequent brain morphometric analysis are inevitably affected by noise. The purpose of this study was to evaluate the effectiveness of an artificial intelligence (AI)-based post-scan processing denoising system, intelligent Quick Magnetic Resonance (iQMR), on MR image quality and brain morphometric analysis.

Methods: We used 1.5T MP-RAGE MR images acquired from the Alzheimer's Disease Neuroimaging Initiative 1 database. The images of 21 subjects were used for cross-sectional analysis and 15 for longitudinal analysis. In the longitudinal analysis, two timepoints over a 2-year interval were used. Each subject was scanned twice at each timepoint. MR images processed with and without the denoising system were compared both visually and objectively using FreeSurfer cortical thickness analysis.

Results: The denoising system reduced the noise with good white–gray matter contrast (noise: $p < 0.001$; contrast: $p = 0.49$). The mean intraclass correlation coefficients (ICCs) of cortical thickness were slightly better in the images processed with the denoising system (0.739/0.859/0.883; Gaussian smoothing kernel of full width at half maximum = 0/10/20) compared with the unprocessed images (0.718/0.854/0.880). In the longitudinal analysis, the mean ICCs of symmetrized percent change improved in images processed with the denoising system (0.202/0.349/0.431) compared with the unprocessed images (0.167/0.325/0.404). In addition, the detectability of significant cortical thickness atrophy improved with denoising.

Conclusion: We confirm that the AI-based denoising system could effectively reduce the noise while retaining the contrast. We also confirm the improvement of the reliability and detectability of brain morphometric analysis with the denoising system.

Introduction

Brain morphometric analysis has become increasingly crucial for the diagnosis and evaluation of various neurodegenerative and psychiatric disorders.[1–3] In Alzheimer's disease, for example, the longitudinal atrophy rate has been used as a biomarker for monitoring disease progression, predicting prognosis, and evaluating the efficacy of disease-modifying therapeutics.[2, 4–6] High-contrast three-dimensional MR images are an excellent way to differentiate gray and white matter and detect disease-related changes. Recent advances in mathematical and computational technology have also made brain morphometric analysis easier, more reliable, and more robust.

However, brain MR images are often affected by various quality deteriorations. Poor image quality affects the accuracy of morphometric analysis, deteriorating its reliability and resulting in its poor credibility as a biomarker. To use morphometric analysis as a reliable and robust biomarker, high-quality MR images are essential. In order to improve image quality, several imaging correction techniques have been proposed, such as N3/N4 bias field correction[7] to reduce residual inhomogeneity and Gradwarp for correction of geometric distortion due to gradient non-linearity.[8]

One important imaging correction technique is denoising. Particularly, post-scan processing denoising techniques have the advantage of not increasing the acquisition time and, therefore, several post-scan processing denoising techniques have been introduced, such as non–local means,[9] singular value decomposition,[10] sparse representation,[11] machine learning-based techniques, and combinations of these.[12]

Intelligent Quick Magnetic Resonance (iQMR; Medic Vision Imaging Solutions, Tirat Carmel, Israel[13]) is a post-scan processing

Abbreviations: FWHM, full width at half maximum; iQMR, intelligent Quick Magnetic Resonance; ICC, intraclass correlation coefficient

Data used in preparation of this article were obtained from the Alzheimer's Disease Neuroimaging Initiative (ADNI) database (adni.loni.usc.edu). As such, the investigators within the ADNI contributed to the design and implementation of ADNI and/or provided data but did not participate in analysis or writing of this report. A complete listing of ADNI investigators can be found at: http://adni.loni.usc.edu/wp-content/uploads/how_to_apply/ADNI_Acknowledgement_List.pdf

* Corresponding author at: Department of Radiology, University of Tokyo, Tokyo, 7-3-1 Hongo, Bunkyo-ku, Tokyo 113-8655, Japan.
E-mail address: kanemaru-tky@umin.ac.jp (N. Kanemaru).

https://doi.org/10.1016/j.neurad.2021.11.007
0150-9861/

denoising system based on artificial intelligence (AI)-assisted iterative image reconstruction technology, using parallel processing by multiple Graphic Processing Units. The algorithms are based on Medic Vision's SafeCT algorithms, adapted to handle MRI imagery. The SafeCT algorithms, which provide noise reduction and image enhancement for CT images, has been evaluated and reported in several publications.[14,15] For iQMR, Tanenbaum et al. have reported that, in visual evaluation, denoised images acquired by about 30% shorter protocols were comparable to images acquired by standard protocols,[16] but without quantitative evaluation.

A post-scan processing denoising system like iQMR has the possibility to improve not only MR image quality but also the quality of morphometric analysis. However, its effectiveness in clinical and research practice has been not thoroughly evaluated, and to the best of our knowledge, there have been no reports evaluating the effectiveness of the post-scan processing denoising system on morphometric analysis.

The purpose of this study was to qualitatively and quantitatively evaluate the effect of the AI-based post-scan processing denoising system (iQMR) on image quality and brain morphometric analysis. The fully automated surface-based morphometric analysis software FreeSurfer was used to objectively evaluate the effect of this system on white−gray matter contrast and morphometric analysis. We also evaluated the performance of the median filter, as a representative of classical denoising algorithms, to see the general impact of denoising on MR images.

Materials and methods

AI-based post-scan processing denoising system (iQMR)[13]

iQMR employs statistical priors of noise distribution in volumetric MR images along with state-of-the-art methods for SNR improvement image enhancement and iterative reconstruction, to restore the image detail and quality of MRI scans that were acquired with relatively poor exposure parameters (e.g., fast or low-resolution scans).

The input data set (MR images) is decomposed into 3D patches. These patches are transformed into feature space by calculating multiple features for each image patch. They are then grouped based on a unique similarity measure. Combining the knowledge of similarity between patches, and the noise statistics estimate, the noise and signal are jointly estimated and separated. This process is iterated until certain convergence criteria are achieved.

The performances of the core iterative reconstruction algorithms can be controlled by parameters that affect the resulting images, for example creating softer/sharper images, enhancing edges, etc. A machine-learning module that compares the input images to certain reference images finds the optimal set of processing parameters for a certain input image, so the output result would be as close as possible to said reference. These parameters are then fed to the iterative reconstruction algorithm in order to provide the best output image. The reference images are high-quality images acquired with the same scanner during implementation of iQMR. Additionally, certain filters may be applied for enhancing certain features (e.g., edges) and restoring image "look and feel" to meet specific preferences of the users (radiologists). Finally, the dataset is reconstructed to the required slice thickness.

Subjects

Data were obtained from the Alzheimer's Disease Neuroimaging Initiative (ADNI) database (http://adni.loni.usc.edu). The ADNI was launched in 2003 as a public-private partnership, led by Principal Investigator Michael W. Weiner, MD. The primary goal of ADNI has been to test whether serial magnetic resonance imaging (MRI), positron emission tomography (PET), other biological markers, and clinical and neuropsychological assessment can be combined to measure the progression of mild cognitive impairment (MCI) and early Alzheimer's disease (AD).

The cross-sectional analysis included 21 subjects (5 females and 16 males, mean age = 75.7 ± 6.9 years, age range = 56−86 years) for whom 1.5T and 3.0T MR images on Philips scanners (Philips Medical Systems, Best, The Netherlands) were available (four with Alzheimer's disease, nine with mild cognitive impairment, and eight normal at baseline). The longitudinal analysis included 15 subjects (4 females and 11 males, mean age = 74.6 ± 7.4 years, age range = 58 −86 years) for whom 1.5T and 3.0T MR images on Philips scanners at baseline and 24-month were available (three with Alzheimer's disease, four with mild cognitive impairment, and eight normal at baseline). At each timepoint for each subject, two images of 1.5T MP-RAGE were acquired. Images of 3T were not used in this study.

Image acquisition

Three-dimensional sagittal T1-weighted volumes were downloaded from the public ADNI 1 database. A MP-RAGE sequences was used to acquire the T1-weighted images over 7 min 12 s with the following parameters: TR: 2300 ms, TE: 4 ms, TI: 1000 ms, flip angle: 8°, FOV: 24 cm, slice thickness: 1.2 mm, acquisition matrix: 192 × 192 × 170, acquisition voxel size: 1.28 × 1.28 × 1.20 mm, reconstructed matrix: 256 × 256 × 170, and reconstructed voxel size: 0.94 × 0.94 × 1.20 mm.

Post-scan processing

We processed each image with different denoising techniques, iQMR and median filter. For iQMR denoising, the following parameters were used: filter = default, and emphasis on the edge = low. Then, bias field correction was applied to all the images (original, iQMR-, and median filter-processed images) using the N3 algorithm to reduce residual intensity inhomogeneity.[7, 17, 18]

Visual evaluation of cross-sectional analysis

Two radiologists, who were blind to the type of the denoising technique, separately assessed the image quality of the images without denoising ("Original"), as well as images processed with iQMR ("AI-based denoising") or median filter ("Median filter"). Noise and white−gray matter contrast were scored as excellent, good, poor, or bad. The scoring criteria is shown in Table 1. Then, inter-reader disagreements were resolved by consensus. Only one scan from each subject was included in the visual evaluation.

Cross-sectional automated morphometry analysis with FreeSurfer

Cortical thickness was measured using the FreeSurfer 6.0.1 system (#), which is a publicly available system package for studying cortical and subcortical anatomy using the surface-based approach. Each image was processed with a cross-sectional processing stream in FreeSurfer. Surface detection and segmentation were visually checked for accuracy. Manual edits of surface models were not performed, as the quality of surface models was almost satisfactory. Cortical thickness was smoothed with 0, 10, and 20-mm full width at

Table 1
The scoring criteria used for visual evaluation.

Grading	Noise	White-gray matter contrast
Excellent	No noticeable noise	Clearly separated
Good	Slight noise	Mostly separated
Poor	Adverse effect for interpretation	Partially separated
Bad	Unacceptable	Unacceptable

Table 2
Visual evaluation in the cross-sectional analysis.

$n = 21$	Noise				White–gray matter contrast			
	Excellent	Good	Poor	Bad	Excellent	Good	Poor	Bad
Original	0	17	4	0	11	8	2	0
AI-based denoising	15	5	1	0	15	6	0	0
Median filter	18	2	1	0	1	15	5	0
p value*	$p < 0.001$				$p < 0.001$			

* Friedman test.

half maximum (FWHM) surface-based Gaussian kernel to reduce local variations in the measurements for further analysis.

Longitudinal automated morphometry analysis with FreeSurfer

Using the results from the cross-sectional analysis, a within-subject template from all timepoints was created to build the average subject anatomy for the longitudinal analysis. Then, each timepoint was analyzed using information from the template and individual cross-sectional data runs to initialize several segmentation algorithms. Thus, within-subject variability and variations in the processing procedures could be effectively reduced without altering the between-subject variability.[19]

Statistical analysis

Visual evaluation of cross-sectional analysis

Using the Friedman test, a significant difference was found for noise and contrast among Original, AI-based denoising, and Median filter images. If a significant difference was found, post-hoc pairwise comparisons were performed with Bonferroni correction for multiple comparisons. Significance level was set at $p < 0.05$.

Cross-sectional automated morphometry analysis with FreeSurfer

Vertex-wise intraclass correlation coefficients (ICCs) of cortical thickness were calculated for Original, AI-based denoising, and Median filter images. The ICC is a measure of within-subject relative to between-subject variability.[20, 21] A two-way mixed model, absolute-agreement, single-measurements reliability study was used.

Longitudinal automated morphometry analysis with FreeSurfer

The reliability of cortical thinning was measured with the vertex-wise ICC of symmetrized percent change. Symmetrized percent change was calculated as follows: symmetrized percent change = 100 × (thickness of timepoint2 − thickness of timepoint1) / [(timepoint2 − timepoint1) × 0.5 × (thickness of timepoint1+ thickness of timepoint2)]. A two-way mixed model, absolute-agreement, single-measurements reliability study was used for ICC calculation.

Significant cortical atrophy in symmetrized percent change was assessed using a one-sample t-test. Among the two longitudinal pairs for each subject, the best image quality pair was included in the statistical analysis. Multiple comparison correction was done with vertex-wise false discovery rate using a threshold of $p < 0.05$.

Results

Visual evaluation of cross-sectional analysis

Fig. 1 shows the unprocessed and processed images (Original, AI-based denoising, and Median filter). AI-based denoising reduced the noise while maintaining the white–gray matter contrast. Median filter reduced noise but obscured the details of anatomical structures and blurred the boundaries. Statistically, a significant difference among Original, AI-based denoising, and Median filter was found for noise and white-gray matter contrast ($p < 0.001$ for both, Table 2). The noise was reduced for AI-based denoising compared with Original ($p < 0.001$). The contrast of white–gray matter tended to improve with AI-based denoising compared with Original, but there was no significant difference ($p = 0.49$). Median filter showed the lesser noise than Original ($p < 0.001$), while there was no significant difference between Median filter and AI-based denoising ($p = 1.00$). The white-gray matter contrast was much more obscure in Median filter compared with Original and AI-based denoising ($p < 0.001$ for both).

Cross-sectional analysis of automated cortical thickness

Fig. 2 shows the vertex-wise ICC of cortical thickness in Original, AI-based denoising, and Median filter with different smoothing kernels (0, 10, and 20 mm) mapped to the surface. Fig. 3 shows the plot

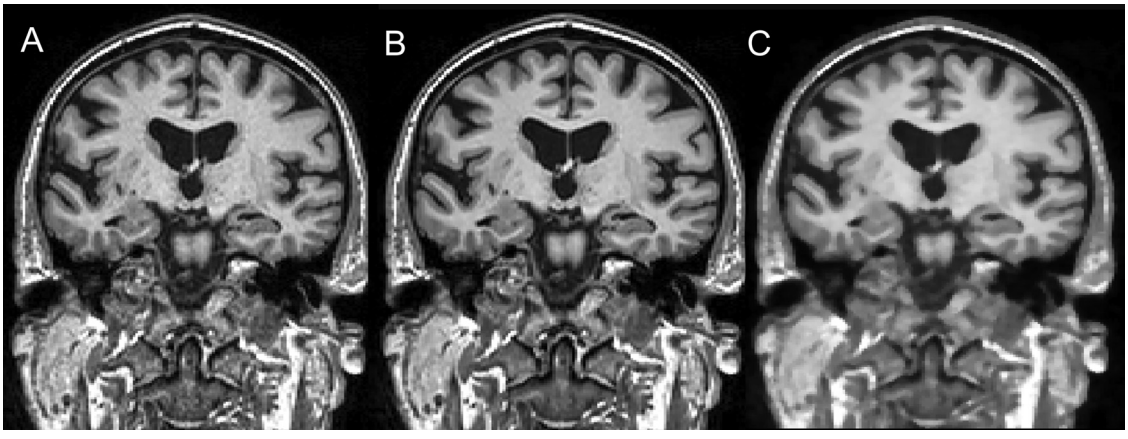

Fig. 1. MR images (A) without denoising, (B) processed with intelligent Quick Magnetic Resonance, and (C) with the median filter.

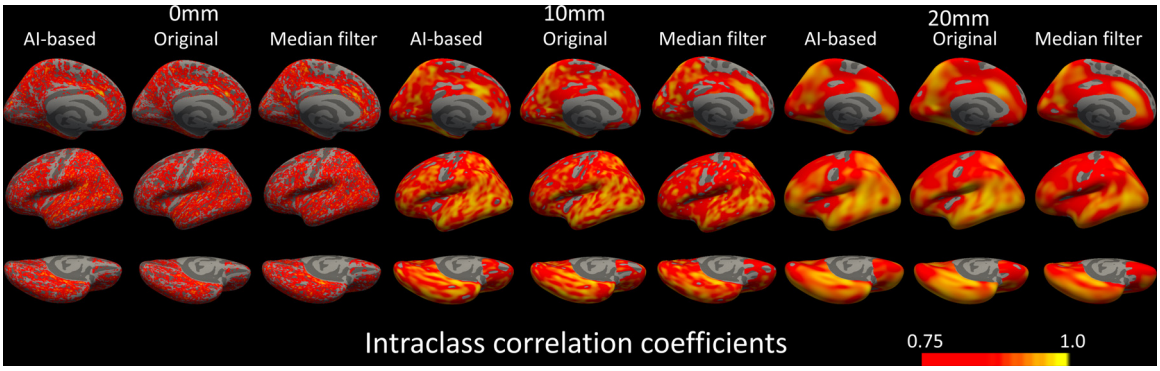

Fig. 2. The intraclass correlation coefficients of the cortical thickness in images without denoising (Original) and processed with intelligent Quick Magnetic Resonance (AI-based denoising) and with the median filter (Median filter) with different smoothing kernels (0, 10, and 20 mm). Due to similarity between hemispheres, only the left hemisphere is shown. Threshold = 0.75−1.0.

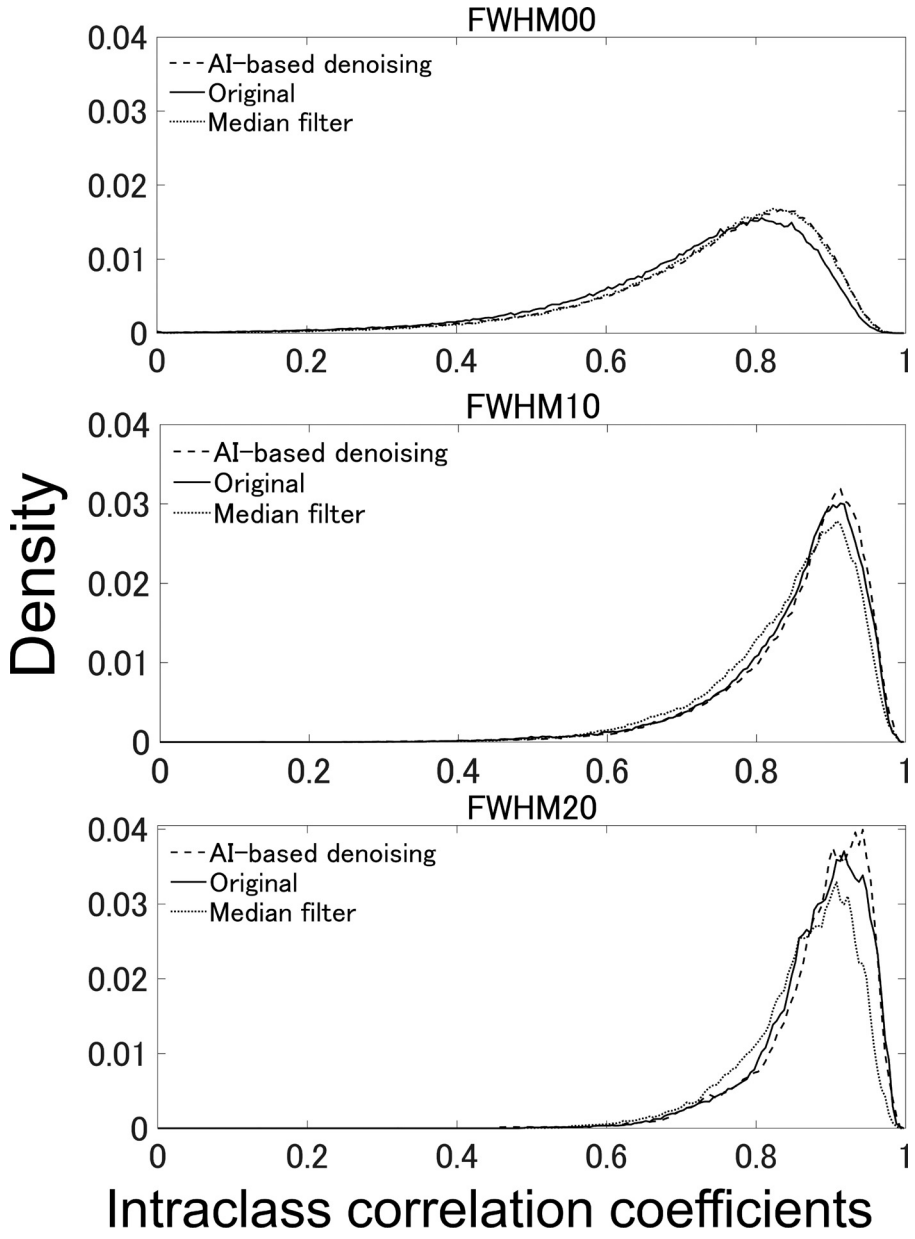

Fig. 3. Plot of the distribution of the intraclass correlation coefficients (ICCs) of the cortical thickness with different smoothing kernels (bin width = 0.005). The ICCs of images processed with the AI-based denoising system (AI-based denoising) tended to be slightly better than images without denoising (Original) and with the median filter (Median filter). FWHM = full width at half maximum.

Table 3
Mean intraclass correlation coefficients (ICCs) of cortical thickness with different FWHMs.

FWHM (mm)	Mean ICC of cortical thickness		
	Original	AI-based denoising	Median filter
0	0.718	0.739	0.741
10	0.854	0.859	0.843
20	0.880	0.883	0.863

FWHM = full width at half maximum.

of the distribution of the ICCs of cortical thickness. Table 3 shows the average ICCs of Original (ICC = 0.718/0.854/0.880), AI-based denoising (ICC = 0.739/0.859/0.883), and Median filter (ICC = 0.741/0.843/0.863) for each FWHM (0/10/20).

Longitudinal analysis of automated cortical thickness

ICC of symmetrized percent change

Fig. 4 shows the vertex-wise ICCs of symmetrized percent change mapped to the surface. The distribution of the ICCs of symmetrized percent change is plotted in Fig. 5. The average ICCs of symmetrized percent change were 0.167/0.325/0.404 in Original and 0.202/0.349/0.431 in AI-based denoising, and 0.200/0.345/0.428 in Median filter for each FWHM (0/10/20) (Table 4).

Significant cortical thinning over 2 years

Fig. 6 shows the significant cortical thinning over 2 years in Original, AI-based denoising, and Median filter. For an FWHM of 20, Original, AI-based denoising, and Median filter showed significant thinning, mainly in the entorhinal and parahippocampal areas. No significant change was detected for an FWHM of 0 or 10. With an FWHM of 20, significant atrophy was observed more widely for AI-based denoising, in the precuneus, frontal, and parietal areas.

Discussion

After processing with the AI-based denoising system, the visual noise was reduced with good white–gray matter contrast. In the cross-sectional and longitudinal morphometric analysis, the ICC of cortical thickness and symmetrized percent change was better in the MR images processed with the AI-based denoising system compared with the images without denoising. In addition, the detectability of significant atrophy was improved by processing with the AI-based denoising system.

Noise and contrast

Denoising methods often remove not only noise but also structural details, such as anatomical boundaries.[22] Thus, we evaluated both noise and white–gray matter contrast to determine if contrast was deteriorated with denoising. The performance of the median filter, one of the major classical denoising techniques, was also evaluated to see the general impact of the denoising on MR images. In addition to visual inspection, we investigated cortical thickness of the images using FreeSurfer. We chose to analyze cortical thickness with FreeSurfer for several reasons. First, we needed a fully automated analysis method to evaluate objectively. Second, among the other measurements and systems, we felt that the surface-based cortical thickness analysis was more sensitive to deterioration in white–gray matter contrast, since a good contrast is essential for the differentiation and segmentation of the white and gray matter and the surface-based approach provides better alignment of cortical landmarks than volume-based registration.[23] Third, since the results could be evaluated per vertex, the variability of the measurement would be increased compared to the volumetric analysis, allowing for easier and more detailed detection of the differences between images with and without denoising. In the visual inspection, the AI-based denoising system reduced the noise with good contrast, while median filter reduced the noise at the cost of the sharpness of the edges and detailed textures. In the cross-sectional and longitudinal analyses using FreeSurfer, the ICCs of cortical thickness were higher in the images with AI-based denoising compared to images without denoising, suggesting that AI-based denoising has a better denoising quality while maintaining contrast.

Comparison of detectability among Original, AI-based denoising, and Median filter

AI-based denoising also showed good detectability in longitudinal changes, reflecting the improvement in ICCs of symmetrized percent change compared to Original and Median filter. For an FWHM of 20, the surface significance map of symmetrized percent change showed stronger and more widespread atrophy in AI-based denoising compared with Original and Median filter, mainly in the entorhinal and parahippocampal areas and extending into the isthmus cingulate and precuneus areas. Those atrophy areas are nearly consistent with a previous report showing prominent atrophy in the mesial and lateral temporal, isthmus cingulate, and orbitofrontal areas in Alzheimer's subjects.[24] For an FWHM of 0 and 10, no significant atrophy area was detected over 2 years. This may be partially because the sample size was not large enough to detect atrophy.

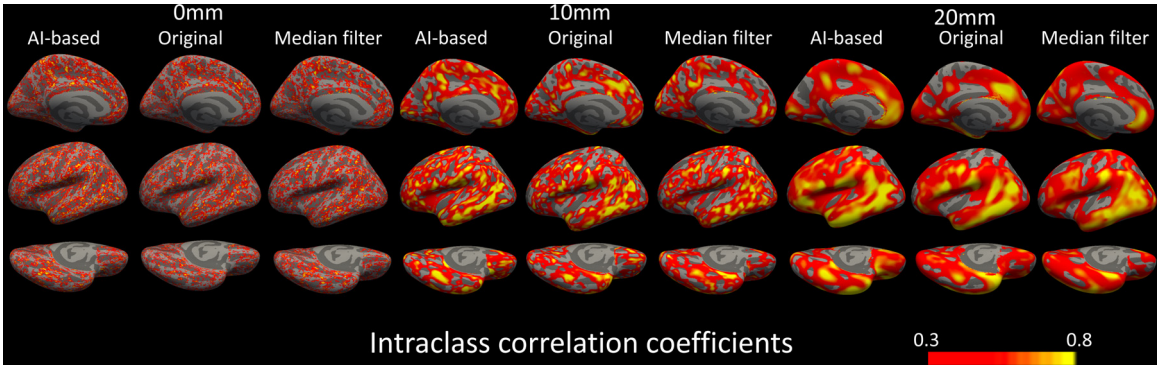

Fig. 4. Vertex-wise intraclass correlation coefficients (ICCs) of symmetrized percent change mapped to the surface. Due to similarity between hemispheres, only the left hemisphere is shown. The ICCs of symmetrized percent change tended to be higher for images processed with the AI-based denoising system (AI-based denoising) compared with images without denoising (Original) and with the median filter (Median filter). Threshold = 0.3–0.8.

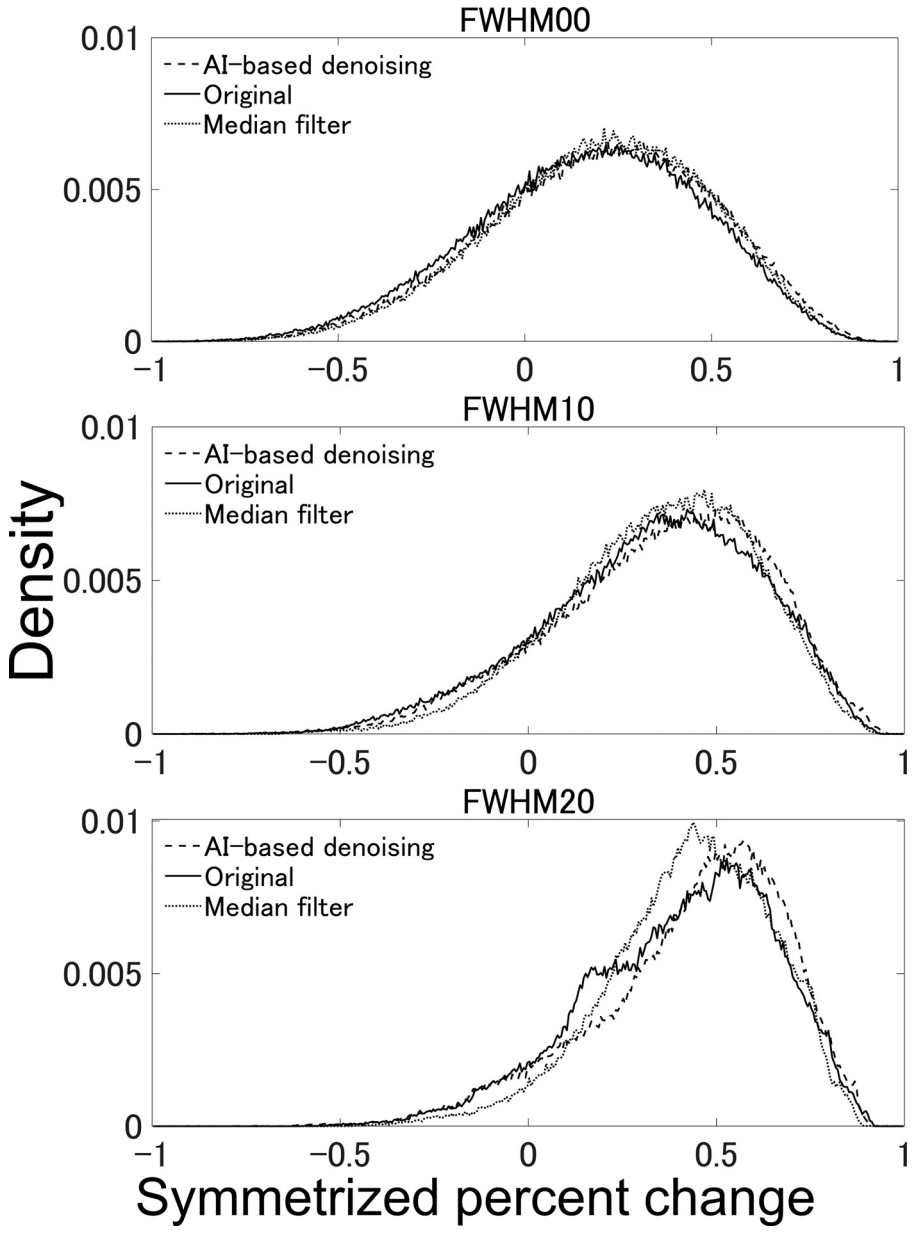

Fig. 5. Plot of the intraclass correlation coefficients (ICCs) of the symmetrized percent change (bin width = 0.005). The ICCs of symmetrized percent change tended to be higher for images processed with the AI-based denoising system (AI-based denoising) compared with images without denoising (Original) and with the median filter (Median filter). FWHM = full width at half maximum.

Table 4
The mean intraclass correlation coefficients (ICCs) of symmetrized percent change with different FWHMs.

FWHM (mm)	Mean ICC of symmetrized percent change		
	Original	AI-based denoising	Median filter
0	0.167	0.202	0.200
10	0.325	0.349	0.345
20	0.404	0.431	0.428

FWHM = full width at half maximum.

The impact of different FWHMs on the morphometric analysis

Previous reports have shown that in cross-sectional cortical thickness analyses, moderate smoothing reduces noise and within-subject variability, resulting in improvement in reliability and detectability, while smoothing also deteriorates spatial resolution, and small local change could be under-estimated when the FWHM was too large.[25–27] A similar trend was observed in our cross-sectional and longitudinal cortical thickness analyses, which showed higher reliability with larger smoothing (FWHM = 0, 10, 20). Additionally, the surface significance map of symmetrized percent change was more widespread for an FWHM of 20 compared to an FWHM of 0 or 10.

Impact of different denoising techniques on morphometric analysis

In cross-sectional analysis, Median filter showed the highest ICC in FWHM = 0 and the lowest ICC in FWHM = 10 and 20. Smoothing improved ICC to a lesser extent in Median filter than in Original and AI-based denoising. This may be because Median filter have less juxta-vertex variability at the cost of the details of anatomical structures, and thus there was less impact of smoothing compared with Original and AI-based denoising.

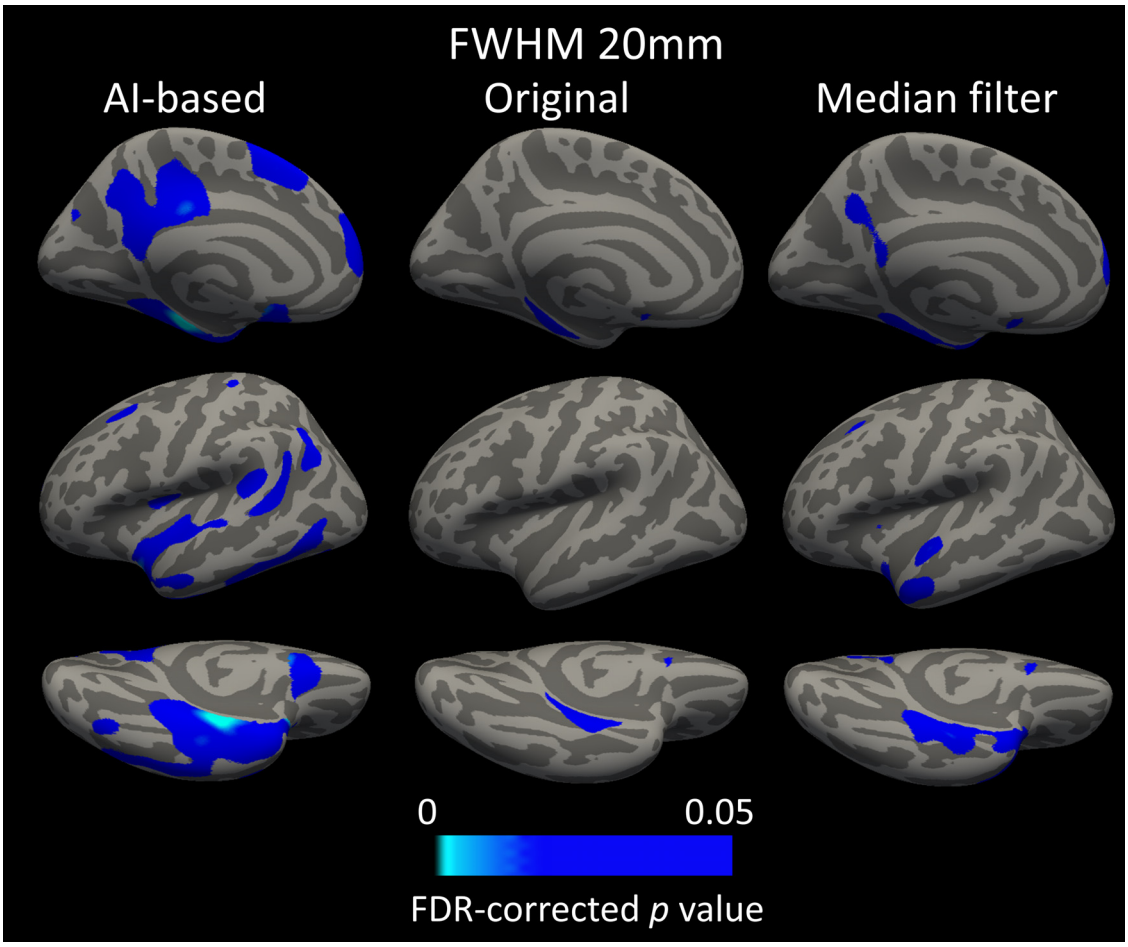

Fig. 6. Significant changes over 2 years for a full width at half maximum (FWHM) of 20. Images without denoising (Original), processed with the AI-based denoising system (AI-based denoising) and processed with the median filter (Median filter) showed a significant decline, mainly in the entorhinal and parahippocampal areas. Significant atrophy was more widely observed for AI-based denoising, in the precuneus, frontal, and parietal areas. FWHM = 0 and 10 are not shown due to no significant changes. Due to similarity between hemispheres, only the left hemisphere is shown. The color scale for statistical difference represents *p* values after false discovery rate correction. Dark and light blue areas represent significant cortical thickness atrophy.

In longitudinal analysis, Median filter showed lower ICC than AI-based denoising and higher ICC than Original. Image processing was initialized with a within-subject template in the longitudinal analysis and a default template in the cross-sectional analysis.[19] Because within-subject templates are created from images at each timepoint, the quality of within-subject templates is also inevitably affected by the quality of each image. Compared with the default template, the use of the within-subject template might be more susceptible to differences in image quality.

Limitations

This study had several limitations. First, the morphometric analysis was done only with FreeSurfer since we felt that surface-based cortical thickness analyses are more sensitive to changes in the white –gray matter contrast. Second, the denoising system was used only for 1.5T MP-RAGE images, and its effectiveness for other sequences or 3.0T images was not assessed in this study. The reason we chose not 3.0T MR images but 1.5T MR images is based on the hypothesis that denoising effects would be more obvious in 1.5T images, which image quality might be lower than 3.0T images. Third, we did not have the ground truth (i.e., postmortem measurements), nor did we know the true atrophy rate. However, the fact that the atrophy areas observed in AI-based denoising were compatible with previous data for Alzheimer's disease and mild cognitive impairment implies a certain degree of reliability.[24] Fourth, the number of the subjects were relatively small (21 subjects for cross-sectional analysis and 15 for longitudinal analysis) since the test-retest data with both 1.5T and 3.0T images on Philips scanners were included in this study. Finally, this study included only the median filter for comparison since we used the median filter to investigate the general impact of denoising on visual image quality and morphometric analysis, rather than to compare the performance between AI-based denoising and other denoising methods.

Conclusions

In conclusion, we confirmed that the AI-based denoising system provides promise for denoising images while retaining contrast, which was verified both visually and objectively using a fully automated morphometric analysis. We also confirmed the improvement in the reliability and detectability of longitudinal analyses in three-dimensional MP-RAGE images.

Funding

The authors did not receive support from any organization for the submitted work.

Conflicts of interest/competing interest

There are no conflicts of interest to disclose.

Availability of date and material

These data were derived from the following resources available in the public domain: the Alzheimer's Disease Neuroimaging Initiative database (adni.loni.usc.edu)

Acknowledgements

Data collection and sharing for this project was funded by the Alzheimer's Disease Neuroimaging Initiative (ADNI) (National Institutes of Health Grant U01 AG024904) and DOD ADNI (Department of Defense award number W81XWH-12-2−0012). ADNI is funded by the National Institute on Aging, the National Institute of Biomedical Imaging and Bioengineering, and through generous contributions from the following: AbbVie, Alzheimer's Association; Alzheimer's Drug Discovery Foundation; Araclon Biotech; BioClinica, Inc.; Biogen; Bristol-Myers Squibb Company; CereSpir, Inc.; Cogstate; Eisai Inc.; Elan Pharmaceuticals, Inc.; Eli Lilly and Company; EuroImmun; F. Hoffmann-La Roche Ltd and its affiliated company Genentech, Inc.; Fujirebio; GE Healthcare; IXICO Ltd.; Janssen Alzheimer Immunotherapy Research & Development, LLC.; Johnson & Johnson Pharmaceutical Research & Development LLC.; Lumosity; Lundbeck; Merck & Co., Inc.; Meso Scale Diagnostics, LLC.; NeuroRx Research; Neurotrack Technologies; Novartis Pharmaceuticals Corporation; Pfizer Inc.; Piramal Imaging; Servier; Takeda Pharmaceutical Company; and Transition Therapeutics. The Canadian Institutes of Health Research is providing funds to support ADNI clinical sites in Canada. Private sector contributions are facilitated by the Foundation for the National Institutes of Health (www.fnih.org). The grantee organization is the Northern California Institute for Research and Education, and the study is coordinated by the Alzheimer's Therapeutic Research Institute at the University of Southern California. ADNI data are disseminated by the Laboratory for Neuro Imaging at the University of Southern California

Reference

1. Pantelis C, Velakoulis D, McGorry PD, et al. Neuroanatomical abnormalities before and after onset of psychosis: a cross-sectional and longitudinal MRI comparison. *Lancet*. 2003;361. https://doi.org/10.1016/S0140-6736(03)12323-9. 281−8.
2. Risacher SL, Shen L, West JD, et al. Longitudinal MRI atrophy biomarkers: relationship to conversion in the ADNI cohort. *Neurobiol Aging*. 2010;31:1401–1418. https://doi.org/10.1016/j.neurobiolaging.2010.04.029.
3. Barnes J, Bartlett JW, van de Pol LA, et al. A meta-analysis of hippocampal atrophy rates in Alzheimer's disease. *Neurobiol Aging*. 2009;30:1711–1723. https://doi.org/10.1016/j.neurobiolaging.2008.01.010.
4. Hua X, Leow AD, Parikshak N, et al. Tensor-based morphometry as a neuroimaging biomarker for Alzheimer's disease: an MRI study of 676 AD, MCI, and normal subjects. *Neuroimage*. 2008;43:458–469. https://doi.org/10.1016/j.neuroimage.2008.07.013.
5. Fennema-notestine C, Jr DJH, Mcevoy LK, et al. Structural MRI Biomarkers for Preclinical and Mild Alzheimer ' s Disease. *Hum Brain Mapp*. 2009;30:3238–3253. https://doi.org/10.1002/hbm.20744.
6. Mcdonald CR, Mcevoy LK, Gharapetian L, et al. Regional rates of neocortical atrophy from normal aging to early Alzheimer disease. *Neurology*. 2009;73:457–465. https://doi.org/10.1212/WNL.0b013e3181b16431.
7. Sled JG, Zijdenbos AP, Evans AC. A nonparametric method for automatic correction of intensity nonuniformity in MRI data. *IEEE Trans Med Imaging*. 1998;17:87–97. https://doi.org/10.1109/42.668698.
8. Jovicich J, Czanner S, Greve D, et al. Reliability in multi-site structural MRI studies: effects of gradient non-linearity correction on phantom and human data. *Neuroimage*. 2006;30:436–443. https://doi.org/10.1016/j.neuroimage.2005.09.046.
9. Buades A, Coll B, Morel J-M. A Non-Local Algorithm for Image Denoising. *2005 IEEE Computer Society Conference on Computer Vision and Pattern Recognition (CVPR'05*. IEEE; 2005:60–65.
10. Manjón JV, Coupé P, Buades A, et al. New methods for MRI denoising based on sparseness and self-similarity. *Med Image Anal*. 2012;16:18–27. https://doi.org/10.1016/j.media.2011.04.003.
11. Elad M, Aharon M. Image denoising via sparse and redundant representations over learned dictionaries. *IEEE Trans Image Process*. 2006;15:3736–3745. https://doi.org/10.1109/tip.2006.881969.
12. Leal N, Zurek E, Leal E. Non-local SVD denoising of MRI based on sparse representations. *Sensors*. 2020;20:1–26. https://doi.org/10.3390/s20051536.
13. iQMR. https://medicvision.com/en/iqmr. Accessed 8 November 2021.
14. Johnson JO, Robins JM. CT imaging: radiation risk reduction−real-life experience in a metropolitan outpatient imaging network. *J Am Coll Radiol*. 2012;9:808–813. https://doi.org/10.1016/j.jacr.2012.06.026.
15. Padole A, Singh S, Ackman JB, et al. Submillisievert chest CT with filtered back projection and iterative reconstruction techniques. *AJR Am J Roentgenol*. 2014;203:772–781. https://doi.org/10.2214/AJR.13.12312.
16. MEDIC VISON. https://medicvision.com/en/mri-scan-time-reduction-asnr-2019-presentation. Accessed 8 November 2021.
17. Takao H, Abe O, Ohtomo K. Computational analysis of cerebral cortex. *Neuroradiology*. 2010;52:691–698. https://doi.org/10.1007/s00234-010-0715-4.
18. Takao H, Abe O, Hayashi N, et al. Effects of gradient non-linearity correction and intensity non-uniformity correction in longitudinal studies using structural image evaluation using normalization of atrophy (SIENA). *J Magn Reson Imaging*. 2010;32:489–492. https://doi.org/10.1002/jmri.22237.
19. Reuter M, Schmansky NJ, Rosas HD, Fischl B. Within-subject template estimation for unbiased longitudinal image analysis. *Neuroimage*. 2012;61:1402–1418. https://doi.org/10.1016/j.neuroimage.2012.02.084.
20. Shrout PE, Fleiss JL. Intraclass correlations: uses in assessing rater reliability. *Psychol Bull*. 1979;86:420–428. https://doi.org/10.1037/0033-2909.86.2.420.
21. McGraw KO, Wong SP. Forming inferences about some intraclass correlation coefficients. *Psychol Methods*. 1996;1:30–46. https://doi.org/10.1037/1082-989X.1.1.30.
22. Fan L, Zhang F, Fan H, Zhang C. Brief review of image denoising techniques. *Vis Comput Ind Biomed*. 2019. https://doi.org/10.1186/s42492-019-0016-7. art 2:7.
23. Mills KL, Tamnes CK. Methods and considerations for longitudinal structural brain imaging analysis across development. *Dev Cogn Neurosci*. 2014;9:172–190. https://doi.org/10.1016/j.dcn.2014.04.004.
24. McEvoy LK, Fennema-Notestine C, Roddey JC, et al. Alzheimer disease: quantitative structural neuroimaging for detection and prediction of clinical and structural changes in mild cognitive impairment. *Radiology*. 2009;251:195–205. https://doi.org/10.1148/radiol.2511080924.
25. Lerch JP, Evans AC. Cortical thickness analysis examined through power analysis and a population simulation. *Neuroimage*. 2005;24:163–173. https://doi.org/10.1016/j.neuroimage.2004.07.045.
26. Han X, Jovicich J, Salat D, et al. Reliability of MRI-derived measurements of human cerebral cortical thickness : the effects of field strength, scanner upgrade and manufacturer. *Neuroimage*. 2006;32:180–194. https://doi.org/10.1016/j.neuroimage.2006.02.051.
27. Liem F, Mérillat S, Bezzola L, et al. NeuroImage Reliability and statistical power analysis of cortical and subcortical FreeSurfer metrics in a large sample of healthy elderly. *Neuroimage*. 2015;108:95–109. https://doi.org/10.1016/j.neuroimage.2014.12.035.